
Munich Personal RePEc Archive

Numerical Investigation of Head Frontal Velocity of nonconservative Dense Flows in Small Inclined Beds

Hajibabaei, Ehsan and Ghasmi, Alireza and Hosseini, Seyed Abbas

Technical and Engineering Department, Science and Research Branch, Islamic Azad University, Tehran, Iran, Technical and Engineering Department, Science and Research Branch, Islamic Azad University, Tehran, Iran, Technical and Engineering Department, Science and Research Branch, Islamic Azad University, Tehran, Iran

February 2017

Online at https://mpra.ub.uni-muenchen.de/88383/
MPRA Paper No. 88383, posted 09 Aug 2018 15:55 UTC

Numerical Investigation of Head Frontal Velocity of Non-conservative Dense Flows in Small Inclined Beds

Ehsan Hajibabaei[1], Alireza Ghasemi[1], Seyed Abbas Hosseini[1]

[1]Technical and Engineering Department, Science and Research Branch, Islamic Azad University, Tehran, Iran

---

Abstract - *Non-conservative dense flow frontal velocity has been simulated two dimensionally by fluent numerical code. The outcomes have been compared with experimental results. Numerical simulation was conducted as two-phase through Euler-Lagrange method. Reynolds-Stress Turbulent Model (RSM) with non-uniform grid and shredding mesh on the channel floor. The results obtained from numerical model of head frontal velocity show a good compliance with experiment results and greatly help analyzing the pattern of fluid movement in different scales.*

Key Words: dense flow, fluent, head frontal velocity

1. INTRODUCTION

The specific area of head is in frontal edge of dense flow that has been deeper than tail area and have different characteristics of flow body. Dynamic identification of head is very important because it is generally considered as a boundary condition for the flow [1]. Dense flows which stream on horizontal surface have almost semi-permanent head and a depth twice the depth of the body of flow but in a flow which passes on a slope, the depth of head always increase. The shape of head in gravity flows aren't generalizable and severely depend on physical conditions, environmental fluid depth and other cases. Figure (1) represents the first experiments that are formed for modeling the head of a cold flow of wind in atmosphere using temperature difference. In figures (1-a) and (1-b), the head of flow with low Reynolds number about 10, $R_{er} = \frac{U_f h_f}{v}$ (U_r head velocity, h_r is its height and v is kinematic viscosity) has been shown. When temperature gets more and the number of Reynolds increases, the form of head will change, its nose gets closer to the earth floor and severe mix occurs in front of and above the head. Figure (1-F) shows a flow whose Reynolds number is upper than 1000 in which some billows raise from high level and goes backwardly [2].

As it can be seen the head of flow is an area in which severe disorder and turbulent happen and there is high density gradient. When velocity and as result the number of Reynolds in flow increase, the form of head changes and mainly turn to more stretched mode. Whirlpool within head during rotation generates many vortices and pollens that in area above that breaks in three dimension and very complicated form and creates some instabilities. The velocity changes may create different types of damages such as erosion, abrasion and cavitation which are extensively reported for concrete and steel structures [3-5]. In head area because of great vortex, turbulence and mixing and inside mixture are also more and gradient of velocity and dense is stronger in this area. Mixture of dense flow with fluid of environment is an important process that occurs in head of flow through dense fluid suction behind and back of head as series of cross vortices [6, 7]. Another example of turbulent flow with hydraulic jump, vortex and pressure fluctuations is considered by Hamedi et al. in stepped spillways with horizontal and inclined steps. They reported that inclination slightly increases the energy loss [8] Hamedi et al., also, mentioned that the combination of inclination and end sill increases the energy loss [9]. Also, velocity field in reservoir has been considered by Sarkardeh et al. in presence of an air-core vortex as another example of turbulent flow [10, 11].

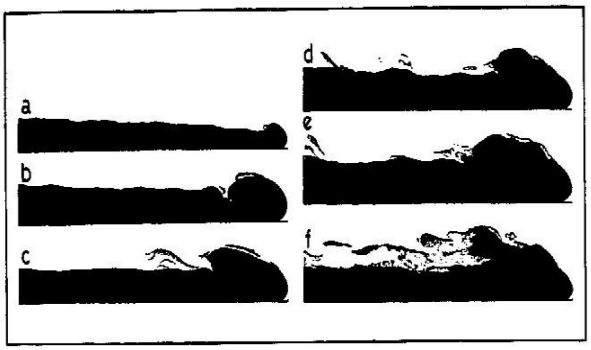

Fig-1: The changes of radial velocity versus time

Figure 1- transformation of head of experiment gravity flow through increasing Reynolds number a) Reynolds number less than 10, f) Reynolds more than 1000 [2]

Using images with slow movement for tracking and following the form of billows in upper boundary of flow show that the wave and range of these billows can grow to the size of head and then they are collapsed and broken [1].

2. Theoretical principles

Dominant equations on the movement of an incompressible viscous fluid at the state of chaos are expressed using averaged Navier-Stokes equations known as Reynolds (RANS). Hamedi et al. mentioned all numerical models which Fluent software is using to solve problems [12]. Continuity equation (conservation of mass) and motion (conservation of momentum) are mentioned below [13]:

- Continuity equation

$$\frac{\partial u_i}{\partial x_i} = 0 \qquad (1)$$

- Momentum equation

$$\frac{\partial u_i}{\partial t} + \frac{\partial u_i u_j}{\partial x_j} = -\frac{1}{\rho}\frac{\partial p}{\partial x_j} + g_i + \frac{\partial}{\partial x_j}\left(\tau_{ij}\right) \qquad (2)$$

U_i is the component of averaged velocity in the time to the direction of x_i, p total pressure, ρ fluid dense, g_i the velocity of gravity to the direction of x_i and τ_{ij} is stress tensor that in turbulent flows, it includes two terms and in addition to the stress caused by average component of flow, the other stress derved from fluctuation component of velocity is created that is known as Reynolds stresses and is shown using Boussinesq's idea.

Modeling in this research id conducted through Euler-Lagrange method so that continuous phase of flow is solved using Euler equations that are Navier-Stokes equations and then second phase for example sedimentary particles are investigated at the points of view of Lagrange; so that the balance of all the forces acting on the particles in two directions of x and y and placing them in the equation of the size of Newton movement F=ma, give the velocity of particle that the position of particle will be found by putting the velocity of particle in the equation of $\frac{d_t}{dx_p}$ that up is the velocity of particle and x_p is spatial position of particle.

Model DPM is one of capabilities of fluent in modeling two-phase flows [16] that its second phase can be formed by sedimentary particles or bubble or drops. Many researches in two-phase flows have noticed this model [16, 17].

3. Initial conditions and numerical solution of equations

In order to solve field of flow and conducting some studies on model, Fluent software has been used. To numerically simulate the dominant equations on these flows, an existing numerical code known as Fluent has been used. Fluent is a strong software in the field of CFD.

Continuity and Navier-Stokes equations are used in analyzing the flow. In case the flow is turbulent then dominant equations turn to Reynolds ones and one-equation, two-equation, five or six-equation models are used for determining eddy viscosity that user determines the type of model [14]. Fluent converts dominant equations to algebraic equations through the method of finite volumes and then solve them.

Considering that Fluent software doesn't generate network itself and the network should be generated in another software, Fluent is capable of reading mesh from other software such as Gambit, Geomesh and ANSIS. In this research in first step, the shape of problem is drawn in AutoCAD software and in the second step, meshing was formed on general geometry in Gambit software [15], meshing is non-uniformly and rectangular. Then the type of the boundaries of solution zone such as wall, input and output were specified, generated mesh is read in Fluent software and controlled in this software in case of probable problems such as negative volumes.
Geometry and boundary conditions of flow have been represented in Figure 2.

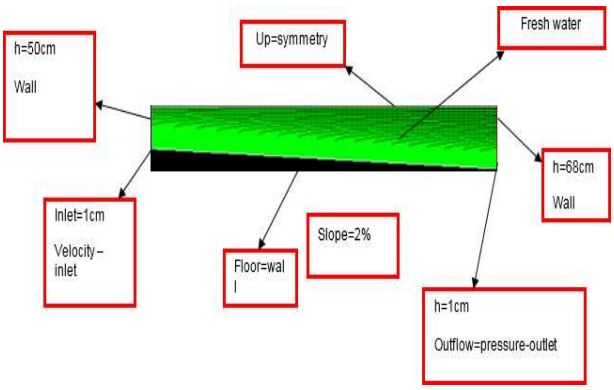

Fig -2: geometry and boundary conditions of flow

For better accordance of results in the section, meshing is fine in 20 centimeters of channel floor that whatever we get closer to the bottom of channel, meshing will be smaller. This meshing method also has been used by Baqersad et al. [18] and Hamedi and Ketabdar [19]. The configuration and topology which was defined by Zeidi et al. [20-23] was helpful to define mesh topology and boundary conditions.

The modeling in this research is two dimensionally. It has to be noticed that spiral movement (helicoidally) is created in two-dimension flows because of non-isotropic turbulent near to walls that can be ignored for wide channels with the ratio of width to higher height than 6 but the velocity of modeling in two-dimension method is more for determining the profile of velocity.

For verifying the results of numerical model, the results of two experiments with slope, flow rates and corresponding concentrations of table 1 were used. Where C_0 is initial concentration, ϱ_0 is dense fluid inflow rate, U_0 the velocity of inflow, b_0 and h_0 are respectively width and height of inlet, g'_0 is the velocity of reduced gravity, B_0 is input floating flux, Re_0 is the number of inflow Reynolds, Ri_0 is initial Richardson number of flow and Fr'_0 is initial Froude number of flow.

The velocity of reduced gravity (g'_0) and input floating flux (B_0) and initial Richardson number (Ri_0) are:

$$g_0^{'} = \frac{\rho - \rho_0}{\rho_0} g \qquad (3)$$

$$B_0 = b_0 . h_0 . U_0 . g_0^{'} \qquad (4)$$

$$Ri_0 = \frac{g_0^{'} . h_0 . \cos\theta}{U_0^2} = \frac{1}{Fr_0^{'2}} \qquad (5)$$

In which fluid dense is dense and water dense is environmental.

Table -1: initial conditions for numerical simulations

RUN.NO	Slope %	C_0 (gr/cm3)	Q_0 (lit/min)	b_0 (cm)	h_0 (cm)	U_0 (cm/s)	g'_0 (cm/s 2)
No.1	2%	0.01	25	20	1	20.83	6.124 5
No.2	2%	0.005	15	20	1	12.50	3.062 5
RUN.NO	B0 (Cm4/s3)	Re_0	Ri_0	Fr'_0			
No.1	127.59	2036.3	0.0141	8.418			
No.2	38.28	1235.0	0.0196	7.143			

4. The results of modeling and comparison with experimental results

How the muddy flow is formed, developed and moved under the flow of stagnant water at different times till when the head reaches the end of channel has been shown in figures 3, 4, 5 and 6. The movement of head and body of a permanent muddy flow have been clearly shown in the figure and t is seen that the height of body is almost fixed but flow head has variable shape and height along the path of channel. Qualitative investigation of characteristics of flow at the time of t=45 and t=120 for slope 2 percent, concentration of 1 percent and flow rate of 25 litter at the time of dense flow coming out at the times of 45 and 120 seconds under the gate have been shown in the following figures.

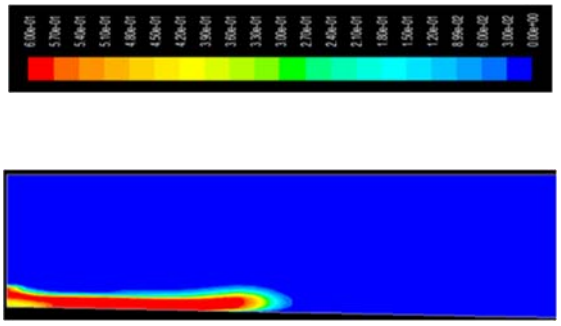

Fig -3: how dense flow moves in channel at the time t=45sec

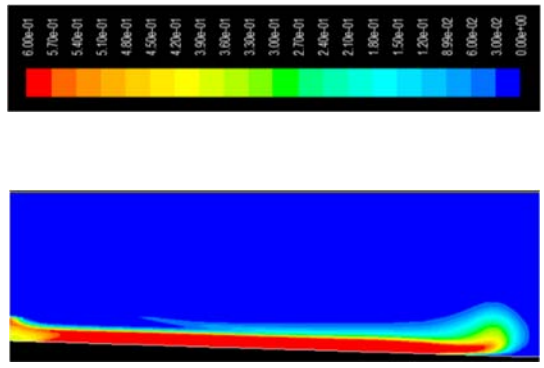

Fig-4: how the dense flow moves in channel at the time of t=120sec

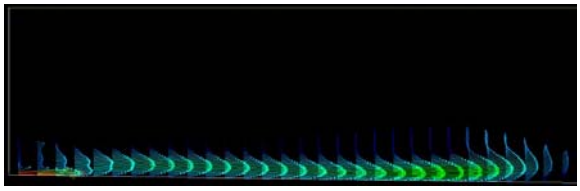

Fig-5: velocity vectors of dense flows at the time t=120sec

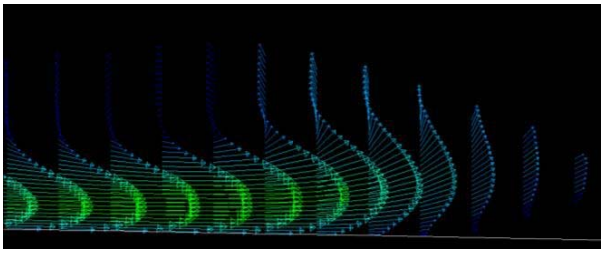

Fig -6: velocity vectors of dense flows in head of flow t=120sec

As following, the head frontal velocity of non-conservative dense flows and the comparison of modeling results with experimental results will be investigated. Being aware of head frontal velocity in dense flows is very important in many engineering functions. Based on this the results of measuring velocity in head of muddy flows which have been obtained using sound velocity meter system by previous experimental researches [1] are used in this part.

How velocity changes, flow frontal velocity in different distances of input using numerical model (fluent) for two experiments have been used in figure 7. As it can be seen at the beginning of input because of created instabilities caused by the sudden withdrawal of dense fluid into environmental fixed fluid, dispersion in measured velocity of fluid front can be justified. In the distance about 3 meters till the end of channel head frontal velocity is fixed. The experimental results, obtained results of frontal velocity in flow head in laboratory and numerical simulation (at the distance of 3 to 11 meters from channel input) have been estimated and compared in figure 8.

In each level of numerical modeling dense flow with specific concentration and flow rate enter the channel from one centimeter down the hatches. When the flow reaches the end of channel, modeling will stop and considering head frontal velocity is fixed in two-dimension flows along channel, it is measured in middle depth of channel and then compared with the relevant experimental results (whose characteristics are in table 1).

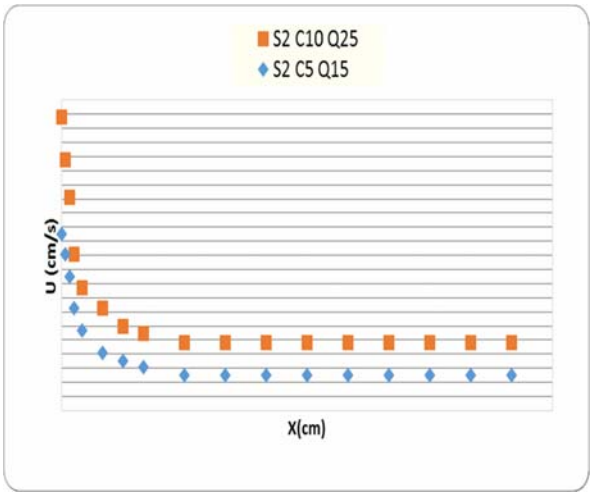

Fig –7: head frontal velocity of dense flows in different distances of input considering obtained numerical model (fluent)

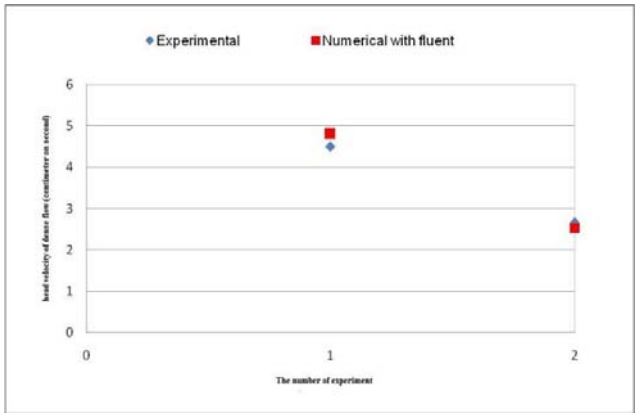

Fig -8: comparing the velocity of head movement of dense flow in numerical model (fluent) with experimental results in the distance of 3 to 11 meter from channel input

Table-2: comparing the velocity of head movement of dense flow in numerical model (fluent) with experimental results

Error	FLUENT	Experiment	Description	Experiment number
6.43	4.8	4.51	S2C10Q25	No.1
-4.89	2.53	2.66	S2C5Q15	No.2

In the distance of 3 to 11 meter from channel input

5. Conclusion

Non-conservative dense flow frontal velocity was simulated in this research using numerical code Fluent through Euler-Lagrange method and was assessed as a suitable tool for hydrodynamic simulation of behavior of experimental dense flows. The comparison of modeling obtained results with experimental results, meanwhile has verified the results of numerical model, it has greatly helped in analyzing the pattern of fluid movement in different scales.

1- Head frontal velocity is fixed considering numerical and experimental modeling in two-dimension mode in distance (3 to 11 meter) from input. Comparing the results of numerical modeling and experimental results, it can be observed that the results have relatively good accordance.
2- The position of forming vortices at the time of passing head and after that can be well observed by numerical model. The areas with high shear stress in the center of dense fluid with environmental fluid can be also observed.
3- Comparing numerical model and experimental data showed that the models of Fluent numerical code that have been established based on CFD can give relatively confident results and is appropriate for simulating this type of flows. Considering the results above, analytical models from turbulent dense flow can be compared with empirical results of this experiment and used with higher confidence coefficient of these models for estimating the volume of sedimentary in channels and reservoirs behind dam and so on.

REFERENCES

[1] A. Soltani-Farani, H. R. Rabiee, and S. A. Hosseini, "Spatial-aware dictionary learning for hyperspectral image classification," *IEEE Transactions on geoscience and remote sensing,* vol. 53, pp. 527-541, 2015.

[2] J. E. Simpson, "Gravity currents in the laboratory, atmosphere, and ocean," *Annual Review of Fluid Mechanics,* vol. 14, pp. 213-234, 1982.

[3] M. Champiri, S. Sajjadi, S. Mousavizadegan, and F. Moodi, "Assessing distress cause and estimating evaluation index for marine concrete structures," *Am. J. Civ. Eng. Arch,* vol. 4, pp. 142-152, 2016.

[4] M. D. Champiri, S. Sajjadi, S. H. Mousavizadegan, and F. Moodi, "A fuzzy system for evaluation of deteriorated marine steel structures," *Journal of Intelligent & Fuzzy Systems,* vol. 32, pp. 1945-1958, 2017.

[5] F. Ghasemzadeh, S. Sajedi, M. Shekarchi, H. Layssi, and M. Hallaji, "Performance evaluation of different repair concretes proposed for an existing deteriorated jetty structure," *Journal of Performance of Constructed Facilities,* vol. 28, p. 04014013, 2013.

[6] J. Allen, "Mixing at turbidity current heads, and its geological implications," *Journal of Sedimentary Research,* vol. 41, pp. 97-113, 1971.

[7] F. Rahmani, F. Razaghian, and A. Kashaninia, "High Power Two-Stage Class-AB/J Power Amplifier with High Gain and Efficiency," 2014.

[8] A. Hamedi, M. Ketabdar, M. Fesharaki, and A. Mansoori, "Nappe Flow Regime Energy Loss in Stepped Chutes Equipped with Reverse Inclined Steps: Experimental Development," *Florida Civil Engineering Journal,* vol. 2, pp. 28-37, 2016.

[9] A. Hamedi, A. Mansoori, A. Shamsai, and S. Amirahmadian, "Effects of End Sill and Step Slope on Stepped Spillway Energy Dissipation," *J. Water Sci. Res., 6 (1), 1,* vol. 15, 2014.

[10] H. Sarkardeh, E. Jabbari, A. R. Zarrati, and S. Tavakkol, "Velocity field in a reservoir in the presence of an air-core vortex," *Proceedings of the Institution of Civil Engineers,* vol. 167, p. 356, 2014.

[11] F. Rahmani, F. Razaghian, and A. Kashaninia, "Novel Approach to Design of a Class-EJ Power Amplifier Using High Power Technology," *World Academy of Science, Engineering and Technology, International Journal of Electrical, Computer, Energetic, Electronic and Communication Engineering,* vol. 9, pp. 541-546, 2015.

[12] A. Hamedi, M. Hajigholizadeh, and A. Mansoori, "Flow Simulation and Energy Loss Estimation in the Nappe Flow Regime of Stepped Spillways with Inclined Steps and End Sill: A Numerical Approach," *Civil Engineering Journal,* vol. 2, pp. 426-437, 2016.

[13] M. Ketabdar and A. Hamedi, "Intake Angle Optimization in 90-degree Converged Bends in the Presence of Floating Wooden Debris: Experimental Development," *Florida Civ. Eng. J,* vol. 2, pp. 22-27.2016, 2016.

[14] M. Ketabdar, "Numerical and Empirical Studies on the Hydraulic Conditions of 90 degree converged Bend with Intake," *International Journal of Science and Engineering Applications,* vol. 5, pp. 441-444, 2016.

[15] A. GAMBIT, "2.2 Tutorial Guide," ed: USA, 2004.

[16] A. N. Georgoulas, P. B. Angelidis, T. G. Panagiotidis, and N. E. Kotsovinos, "3D numerical modelling of turbidity currents," *Environmental fluid mechanics,* vol. 10, pp. 603-635, 2010.

[17] F. K. Purian and E. Sadeghian, "Mobile robots path planning using ant colony optimization and Fuzzy Logic algorithms in unknown dynamic environments," in *Control, Automation, Robotics and Embedded Systems (CARE), 2013 International Conference On*, 2013, pp. 1-6.

[18] M. Baqersad, A. E. Haghighat, M. Rowshanzamir, and H. M. Bak, "Comparison of coupled and uncoupled consolidation equations using finite element method in plane-strain condition," *Civil Engineering Journal,* vol. 2, pp. 375-388,

2016.

[19] A. Hamedi and M. Ketabdar, "Energy Loss Estimation and Flow Simulation in the skimming flow Regime of Stepped Spillways with Inclined Steps and End Sill: A Numerical Model," *International Journal of Science and Engineering Applications,* vol. 5, pp. 399-407, 2016.

[20] S. M. J. Zeidi and M. Mahdi, "Evaluation of the physical forces exerted on a spherical bubble inside the nozzle in a cavitating flow with an Eulerian/Lagrangian approach," *European journal of physics,* vol. 36, p. 065041, 2015.

[21] M. Mahdi, "Investigation the effects of injection pressure and compressibility and nozzle entry in diesel injector nozzle's flow," *Journal of Applied and Computational Mechanics,* vol. 1, pp. 83-94, 2014.

[22] S. Zeidi and M. Mahdi, "Effects of nozzle geometry and fuel characteristics on cavitation phenomena in injection nozzles," in *Proceedings of the 22st Annual International Conference on Mechanical Engineering-ISME*, 2015.

[23] S. Zeidi and M. Mahdi, "Investigation of viscosity effect on velocity profile and cavitation formation in Diesel injector nozzle," in *Proceedings of the 8th International Conference on Internal Combustion Engines*, 2014.